ACS SENSORS

pubs.acs.org/acssensors

Letter

Dipole-Modulated Downconversion Nanoparticles as Label-Free Biological Sensors

Khashayar R. Bajgiran, James A. Dorman,* and Adam T. Melvin*

Cite This: https://dx.doi.org/10.1021/acssensors.9b02204

Read Online

ACCESS | Metrics & More | Article Recommendations | Supporting Information

ABSTRACT: Ultrasensitive detection of proteins and biomolecules has been previously achieved by optical nanoparticles (NPs) using the principles of Förster resonance energy transfer (FRET). However, the inherent need for labeling the target analyte in these assays hinders their applicability in point-of-use (POU) diagnostics. In this work, a label-free NP-based sensor has been developed that utilizes down-conversion luminescence and surface electric dipoles as a novel approach for the detection of avidin. The long-lived luminescence of Eu^{3+}-doped biotinylated NPs was effectively quenched in the presence of avidin in a concentration-dependent manner. The NPs exhibited high avidin selectivity and sensitivity with a limit of detection (LOD) of 7.8 nM and a wide dynamic range spanning 1 nM to 10 μM in deionized (DI) water. The application of the assay in a complex biological matrix consisting of cell growth medium supplemented with 10% v/v serum was verified with minor effects on avidin sensitivity exhibited by an LOD of 34.7 nM. The performance of the system was evaluated by comparing the photoluminescence (PL) intensities of known avidin concentration and the values predicted by the generated calibration curve. The new biosensing strategy has the potential to be extended to the detection of other disease biomarkers or pathogens with LOD and limited matrix effects in POU settings.

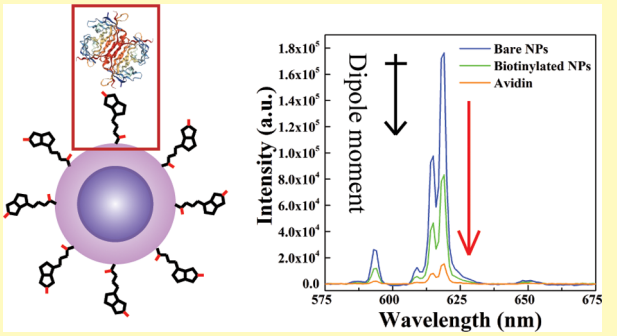

KEYWORDS: *fluorescent biosensor, dipole moment, label-free, biotin, avidin*

Downloaded via BIU SANTE on January 13, 2020 at 10:32:30 (UTC).
See https://pubs.acs.org/sharingguidelines for options on how to legitimately share published articles.

Traditional diagnostic approaches such as the enzyme-linked immunosorbent assay (ELISA) enable the capture and detection of proteins through antibody−antigen binding interactions, while oligonucleotide microarray and sequencing technologies (e.g., polymerase chain reaction-PCR) allow for the identification and discovery of specific nucleic acid targets.[1,2] While these approaches possess high sensitivity (LOD within fM−pM range) and selectivity, they lack multiplexing capabilities, require large volumes of reagents, contain multiple time-consuming processing steps, and require highly trained personnel for assay operation.[3−5] Therefore, conventional methods are incompatible with the growing need for POU diagnostics according to the set of criteria summarized by the acronym ASSURED (Affordable, Sensitive, Specific, User-friendly, Robust and rapid, Equipment-free, Deliverable) proposed by the World Health Organization (WHO).[6] Several optically based techniques have been developed to bypass the challenges encountered with traditional bioassays.[7,8] Specifically, a growing body of optical sensors utilize the FRET effect where the sensor sensitivity is highly dependent on the structure and efficiency of the fluorophore energy donor.[9−11] Numerous drawbacks of commonly used organic dyes, including photobleaching, blinking effects, and sample interference, make them unsuitable energy donors.[12−14] Semiconductor quantum dots (QDs) have been favorably adopted in the FRET-based studies due to their distinct optical characteristics such as tunable size-dependent emission, high PL quantum yields, broad excitation spectra, and narrow emission bandwidths.[15,16] However, their inherent toxicity and chemical instability limit their application in biological detection and medical diagnosis.[17,18] Compared to organic dyes and QDs, rare earth (RE)-doped luminescent NPs exhibit superior features, including long luminescence lifetime (μs−ms range), large (anti)Stokes shifts (>50 nm), narrow emission bandwidths (<10 nm), low toxicity, and high resistance to photobleaching, which has led to their use as energy donors.[19−21] Regardless of the type of energy donor/acceptor, the majority of FRET-based assays require fluorescent labeling of the target analyte. This makes a bioanalytical assay vulnerable to changes in pH, temperature, ionic concentration, and oxidation, limiting their utility for POC applications.[22,23]

To address the challenges of current FRET-based sensors, Bajgiran et al. recently developed a Bi^{3+}-doped YVO_4:Eu^{3+}|YVO_4:Bi^{3+} core−shell (CS) nanoarchitecture that exhibits

Received: November 8, 2019
Accepted: January 6, 2020
Published: January 6, 2020

© XXXX American Chemical Society

adaptive downconversion (DC) luminescence upon modification with weak electric surface ligands.[24] The hybridization of the Bi^{3+}/VO_4^{3-} energy levels was observed to be a function of the weak electric dipole generated by the surface decorated ligand. This difference in the hybridization in the presence of ligands of the Bi^{3+}/VO_4^{3-} energy levels resulted in changes in energy level overlap between Bi^{3+}/VO_4^{3-} and Eu^{3+} ions, altering the luminescence. Ultimately, tuning of the hybridization resulted in a systematic enhancement or quenching of the luminescent signal based on the direction and magnitude of the dipole moment.[24] In the present study, the label-free detection of avidin is demonstrated through the dipole modulation of the developed CSNPs surface functionalized with biotin to exploit the well-established biotin−avidin interactions (Scheme 1). The biotin−avidin complex has

Scheme 1. Illustration of the Sensing Mechanism Harnessing the Changes in Dipole Moment at the Surface of the Nanoparticle Sensor

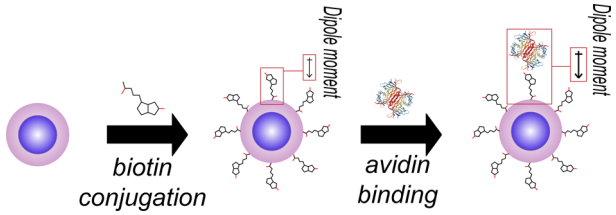

been adopted extensively to characterize novel bioanalytical and biotechnological applications because of its high affinity ($\sim 7.0 \times 10^{14}$ M^{-1}) leading to stable biomolecular constructs.[25−29] Functionalizing the surface of the CSNPs with D-biotin initially generated a positive dipole moment (i.e., electron-withdrawing), resulting in a decreased luminescent signal (Figure S1A). The high affinity between the tetrameric protein avidin and the vitamin biotin applied a larger positive dipole moment at the surface of the CSNPs resulting in further quenching of the luminescence.

The surface of the CSNPs was functionalized with biotin using carboxylic acid chemistry[30] instead of capping ligands or cross-linking agents, both of which require complex reaction chemistries. Fourier-transform infrared spectroscopy (FTIR) verified the successful conjugation of biotin to the CSNP surface by exhibiting the presence of a sharp peak at 1686 cm^{-1} in the spectrum of the functionalized CSNPs, assigned to the stretching vibration of the amide bond (Figure S1B).[31] As a result of surface modification, the zeta-potential for CSNP colloidal solution (pH = 6.99) changed markedly from −26.8 to −38.9 mV after biotinylation (Figure S1C). The highly negative zeta-potential values stabilize the CSNP colloids by means of electrostatic repulsion. Accordingly, these biotinylated CSNPs exhibit superior DI water dispersity compared to nonfunctionalized CSNPs by forming a more transparent colloidal solution that can be easily observed with the naked eye (Figure S1D). In order to properly characterize avidin detection, the surface coverage of the biotin functionalized CSNPs was measured to be 0.35 $\mu mol.mg^{-1}$ based on the thermogravimetric analysis (TGA) performed on the biotinylated CSNPs (Figure S1E).

The biotinylated CSNPs were titrated against various concentrations of avidin (1.0 nM to 10 μM) dispersed in DI water to monitor concentration-dependent changes in the PL intensity. After 5 min of incubation, gradual quenching of the PL intensity was detected with increasing avidin concentration due to the larger positive dipole applied at the local surface of the CSNPs through avidin−biotin interactions (Figure 1A). A

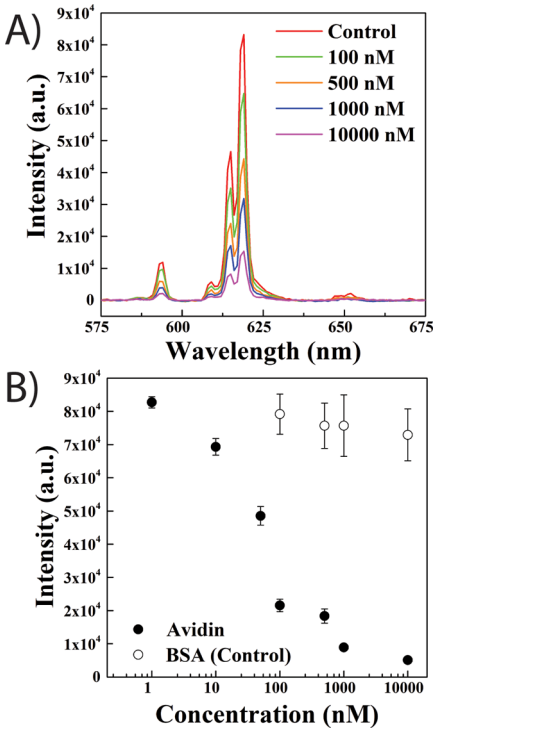

Figure 1. Biotinylated CSNPs can detect avidin at low LODs in DI water. (A) 0.1 mg/mL of biotinylated CSNPs were incubated with different avidin concentrations in DI water for 5 min resulting a significant PL quenching. Control indicates biotinylated CSNP in DI water. (B) Calibration curve determined the LOD of the biotinylated CSNPs was 7.8 nM. Control indicates biotinylated CSNPs in DI water at the presence of BSA.

standard calibration curve was generated after 30 min of incubation to form a basis for reliably determining the amount of free avidin in solution (Figure 1B). Plotting the intensity of Eu^{3+} emission (positioned at 619 nm) as a function of the logarithm of avidin concentration exhibited a wide dynamic range of 1 nM to 10 μM with strong linearity ($R^2 = 0.99$) over 10−100 nM range. Using this response, the LOD for the avidin system was determined to be 7.8 nM (Figure S2A), which is comparable to those of QD/UC FRET-based methods (LOD = 0.5−10 nM).[31−33] It should be noted that the avidin used in this work is not conjugated to a fluorescent tag, and therefore, it has minimal light absorption within the emission (~619 nm) and excitation (~300 nm) range of the CSNPs (Figure S3A). The avidin light absorption within these ranges is not concentration-dependent. Thus, there is minimal energy absorption by avidin at the excitation/emission wavelength range of the CSNPs, which is in contrast with the sensing mechanism of a typical FRET-based assay.[10,34] Furthermore, it is well-known that in addition to excitation/emission intensity, the luminescence lifetime of the NP phosphor also changes in FRET-based assays.[10,34] In order to clearly distinguish between the sensing mechanism proposed in this work and other FRET-based assays, the emission lifetime of the Eu^{3+} was monitored with increasing concentrations of avidin. As can be seen from Figure S3B and Table S1, in contrast to FRET-based assays,[34] there are no discernible changes between the

https://dx.doi.org/10.1021/acssensors.9b02204
ACS Sens. XXXX, XXX, XXX−XXX

emission lifetimes of the CSNPs in the absence or presence of the avidin.

To examine whether the observed changes in the PL intensity of biotinylated CSNPs were due to avidin binding, the changes in the PL intensity of the CSNPs were monitored in the presence of increasing concentrations (0.1−10 μM) of bovine serum albumin (BSA) in DI water (Figure S4A). Negligible BSA interference was observed in the PL intensity after 5 min of incubation, suggesting superior selectivity of the avidin sensing assay. Furthermore, nonfunctionalized CSNPs were incubated with increasing avidin concentrations (0.1−10 μM) for 5 min to ensure that the presence of biotin at the CSNP surface is required for the detection mechanism (Figure S4B). The PL intensity of the nonfunctionalized CSNPs was generally higher compared to the biotinylated CSNPs due to changes in the dipole moment applied at the surface of the CSNPs at the presence of biotin. Nonetheless, no apparent changes in the PL intensity were observed after adding the avidin to the nonfunctionalized CSNPs, confirming that the PL quenching is due to specific biotin−avidin interactions. Next, titration experiments were conducted to assess the effect of biotinylated CSNPs concentrations (50−500 μg/mL) in the detection of a single concentration (1 μM) of avidin. This was done to demonstrate the wide range of concentrations that can be adopted by CSNPs for avidin detection. As expected, the PL intensity of Eu^{3+} emission increased with increasing concentrations of the biotinylated CSNPs (Figure S5) suggesting the tunability of the sensing platform signal-to-noise ratio (SNR) and LOD. These findings support the promise of the CSNPs as novel biosensors possessing high specificity and selectivity.

The versatility of the CSNPs for avidin detection was further investigated by monitoring the performance of the biotinylated NP sensor in complex biological samples (mammalian cell growth media: DMEM + 10% v/v fetal bovine serum, FBS). A concentration-dependent decrease in the PL intensity of CSNPs was similarly observed in DMEM + 10% v/v FBS (Figure 2A). The SNR of the biotinylated NP was found to be lower in the complex biological matrix compared to DI water and FBS-free DMEM solution (Table S2); however, the SNR values were still within the range of competing NP-based biosensors.[35,36] A calibration curve of avidin detection for the CSNPs in the complex media exhibited the same shape as the one observed in DI water (Figure 2B). The addition of avidin did result in a slight increase of the calculated LOD (34.7 nM, Figure S2B); however, this small single order of magnitude change was low compared to the matrix effects of competing bioanalytical sensors.[37]

The accuracy of the CSNP system was evaluated for avidin monitoring in both DI water and serum spiked DMEM solutions by comparing the intensity values of known avidin concentrations (80 and 800 nM) to values predicted from the generated calibration curves (Table 1, Table S3, and Figure S6). Calibration curves for avidin detection by CSNPs were fitted to logistic sigmoid curves and the observed intensity values were calculated from the fitted equations (see Supporting Information). The coefficient of variance (CV), defined as the ratio of the standard deviation to the mean, was less than 10% for all cases (except 80 nM avidin test in DMEM media, 12.8%) which confirms the robustness of the generated calibration curves. The 80 nM avidin test in DMEM + 10% FBS media has a higher CV due to the increased susceptibility of the CSNPs to serum-induced matrix effects at low avidin concentrations, as also evident from the increased LOD.[34]

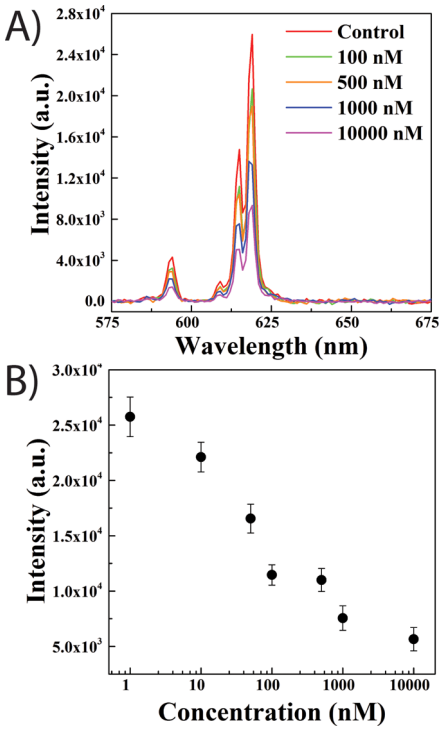

Figure 2. Matrix effects on the performance of biotinylated CSNPs. (A) 0.1 mg/mL of biotinylated CSNPs was incubated with different avidin concentrations in DMEM + 10% FBS for 5 min resulting a significant PL quenching. Control indicates biotinylated CSNPs in DMEM+10% FBS with no avidin. (B) Calibration curve determined the LOD of the biotinylated CSNPs was 34.7 nM.

Table 1. Statistical Analysis on the Performance of the CSNPs to Measure Known Avidin Concentrations (with 0.1 mg/mL CSNP Concentration)

solution	avidin concentration (nM)	calculated intensity (a.u.)	measured intensity (a.u.)	CV (%)
DI Water	80	31240	27500	9
	800	10020	8762	9.5
DMEM + 10% FBS	80	13270	10250	12.8
	800	8270	9304	5.9

These results demonstrate the potential applicability of using the CSNPs for POU monitoring of analytes and biomolecules in a range of settings with good resistivity to matrix effects, which is considered a major bottleneck for existing biosensors.[38]

In summary, novel downconversion CSNPs that utilize the changes in local surface dipole as a sensing mechanism have been reported for avidin detection. Benefiting from the specific interactions between avidin and biotinylated CSNPs, this approach exhibits high sensitivity (LOD = 7.8 nM) and selectivity without the need for target analyte labeling. The sensor performance was tested in a complex biological matrix, where good LOD (34.7 nM) and SNR (11.7) were achieved. The robustness of the system was verified by comparing the PL intensity from a known concentration of avidin and the values predicted by the calibration curve. Due to the hydrophilic nature of the CSNP surface, it is believed that the surface functionalization should be straightforward for most biomolecules using established functionalization methods. It should also be noted that the dipole induced external field is

https://dx.doi.org/10.1021/acssensors.9b02204
ACS Sens. XXXX, XXX, XXX−XXX

a surface effect, not suitable for larger CSNPs.[39] While it is believed that this mechanism will be suitable for other biological systems, these systems need to be examined (experimentally or via simulation) to quantify the effective dipole moment and luminescent response. Overall, this inexpensive and label-free NP sensor has the potential to be coupled with different surface ligands for the detection of small molecules, enzymes, antibodies, and aptamers with high sensitivity and reliability in clinical and POU diagnosis settings.

■ ASSOCIATED CONTENT

Supporting Information

The Supporting Information is available free of charge at https://pubs.acs.org/doi/10.1021/acssensors.9b02204.

Details on CSNP synthesis, surface functionalization, and characterization as well as assay development and statistical analysis (PDF)

■ AUTHOR INFORMATION

Corresponding Authors

James A. Dorman − *Louisiana State University, Baton Rouge, Louisiana;* orcid.org/0000-0002-3248-7752; Email: jamesdorman@lsu.edu

Adam T. Melvin − *Louisiana State University, Baton Rouge, Louisiana;* orcid.org/0000-0003-0484-5871; Email: melvin@lsu.edu

Other Author

Khashayar R. Bajgiran − *Louisiana State University, Baton Rouge, Louisiana*

Complete contact information is available at: https://pubs.acs.org/10.1021/acssensors.9b02204

Notes

The authors declare no competing financial interest.

■ ACKNOWLEDGMENTS

This work was partially supported by the Louisiana Board of Regents, LEQSF(2016-19)-RD-A-03 (JAD). The authors would like to thank Dr. Bhuvnesh Bharti (LSU) and Mr. Jin Gyun Lee (LSU) for aiding with zeta-potential measurements and Mr. Joseph Balhoff (LSU) for help with drawing the images in Scheme 1.

■ REFERENCES

(1) Chen, Z. P.; Wang, H.; Zhang, Z. Y.; Chen, L. X. Chemical Redox-Cycling for Improving the Sensitivity of Colorimetric Enzyme-Linked Immunosorbent Assay. *Anal. Chem.* **2019**, *91* (2), 1254−1259.

(2) Chen, X.; Ba, Y.; Ma, L. J.; Cai, X.; Yin, Y.; Wang, K. H.; Guo, J. G.; Zhang, Y. J.; Chen, J. N.; Guo, X.; Li, Q. B.; Li, X. Y.; Wang, W. J.; Zhang, Y.; Wang, J.; Jiang, X. Y.; Xiang, Y.; Xu, C.; Zheng, P. P.; Zhang, J. B.; Li, R. Q.; Zhang, H. J.; Shang, X. B.; Gong, T.; Ning, G.; Zen, K.; Zhang, J. F.; Zhang, C. Y. Characterization of microRNAs in serum: a novel class of biomarkers for diagnosis of cancer and other diseases. *Cell Res.* **2008**, *18* (10), 997−1006.

(3) Baker, M. MicroRNA profiling: separating signal from noise. *Nat. Methods* **2010**, *7* (9), 687−692.

(4) Goodwin, S.; McPherson, J. D.; McCombie, W. R. Coming of age: ten years of next-generation sequencing technologies. *Nat. Rev. Genet.* **2016**, *17* (6), 333−351.

(5) Dasilva, N.; Diez, P.; Matarraz, S.; Gonzalez-Gonzalez, M.; Paradinas, S.; Orfao, A.; Fuentes, M. Biomarker Discovery by Novel Sensors Based on Nanoproteomics Approaches. *Sensors* **2012**, *12* (2), 2284−2308.

(6) Pai, N. P.; Vadnais, C.; Denkinger, C.; Engel, N.; Pai, M. Point-of-Care Testing for Infectious Diseases: Diversity, Complexity, and Barriers in Low- And Middle-Income Countries. *Plos Medicine* **2012**, *9* (9), e1001306.

(7) Russell, S. M.; Domenech-Sanchez, A.; de la Rica, R. Augmented Reality for Real-Time Detection and Interpretation of Colorimetric Signals Generated by Paper-Based Biosensors. *Acs Sensors* **2017**, *2* (6), 848−853.

(8) Chang, H. J.; Kang, H. M.; Ko, E.; Jun, B. H.; Lee, H. Y.; Lee, Y. S.; Jeang, D. H. PSA Detection with Femtomolar Sensitivity and a Broad Dynamic Range Using SERS Nanoprobes and an Area-Scanning Method. *Acs Sensors* **2016**, *1* (6), 645−649.

(9) Suzuki, M.; Husimi, Y.; Komatsu, H.; Suzuki, K.; Douglas, K. T. Quantum dot FRET Biosensors that respond to pH, to proteolytic or nucleolytic cleavage, to DNA synthesis, or to a multiplexing combination. *J. Am. Chem. Soc.* **2008**, *130* (17), 5720−5725.

(10) Shi, J. Y.; Tian, F.; Lyu, J.; Yang, M. Nanoparticle based fluorescence resonance energy transfer (FRET) for biosensing applications. *J. Mater. Chem. B* **2015**, *3* (35), 6989−7005.

(11) Gao, L.; Lian, C. Q.; Zhou, Y.; Yan, L. R.; Li, Q.; Zhang, C. X.; Chen, L.; Chen, K. P. Graphene oxide-DNA based sensors. *Biosens. Bioelectron.* **2014**, *60*, 22−29.

(12) Smith, A. M.; Nie, S. M. Semiconductor Nanocrystals: Structure, Properties, and Band Gap Engineering. *Acc. Chem. Res.* **2010**, *43* (2), 190−200.

(13) Ha, T.; Tinnefeld, P. Photophysics of Fluorescent Probes for Single-Molecule Biophysics and Super-Resolution Imaging. *Annu. Rev. Phys. Chem.* **2012**, *63*, 595−617.

(14) Cannone, F.; Chirico, G.; Bizzarri, A. R.; Cannistraro, S. Quenching and blinking of fluorescence of a single dye molecule bound to gold nanoparticles. *J. Phys. Chem. B* **2006**, *110* (33), 16491−16498.

(15) Clapp, A. R.; Medintz, I. L.; Mauro, J. M.; Fisher, B. R.; Bawendi, M. G.; Mattoussi, H. Fluorescence resonance energy transfer between quantum dot donors and dye-labeled protein acceptors. *J. Am. Chem. Soc.* **2004**, *126* (1), 301−310.

(16) Maxwell, D. J.; Taylor, J. R.; Nie, S. M. Self-assembled nanoparticle probes for recognition and detection of biomolecules. *J. Am. Chem. Soc.* **2002**, *124* (32), 9606−9612.

(17) Wang, Y. C.; Hu, R.; Lin, G. M.; Roy, I.; Yong, K. T. Functionalized Quantum Dots for Biosensing and Bioimaging and Concerns on Toxicity. *ACS Appl. Mater. Interfaces* **2013**, *5* (8), 2786−2799.

(18) Gai, S. L.; Li, C. X.; Yang, P. P.; Lin, J. Recent Progress in Rare Earth Micro/Nanocrystals: Soft Chemical Synthesis, Luminescent Properties, and Biomedical Applications. *Chem. Rev.* **2014**, *114* (4), 2343−2389.

(19) Goldys, E. M.; Drozdowicz-Tomsia, K.; Sun, J. J.; Dosev, D.; Kennedy, I. M.; Yatsunenko, S.; Godlewski, M. Optical characterization of Eu-doped and undoped Gd2O3 nanoparticles synthesized by the hydrogen flame pyrolysis method. *J. Am. Chem. Soc.* **2006**, *128* (45), 14498−14505.

(20) Vaithiyanathan, M.; Bajgiran, K. R.; Darapaneni, P.; Safa, N.; Dorman, J. A.; Melvin, A. T. Luminescent nanomaterials for droplet tracking in a microfluidic trapping array. *Anal. Bioanal. Chem.* **2019**, *411* (1), 157−170.

(21) Nichkova, M.; Dosev, D.; Gee, S. J.; Hammock, B. D.; Kennedy, I. M. Microarray immunoassay for phenoxybenzoic acid using polymer encapsulated Eu: Gd2O3 nanoparticles as fluorescent labels. *Anal. Chem.* **2005**, *77* (21), 6864−6873.

(22) Li, T. H.; Jeon, K. S.; Suh, Y. D.; Kim, M. G. A label-free, direct and noncompetitive FRET immunoassay for ochratoxin A based on intrinsic fluorescence of an antigen and antibody complex. *Chem. Commun.* **2011**, *47* (32), 9098−9100.

(23) Leavesley, S. J.; Rich, T. C. Overcoming Limitations of FRET Measurements. *Cytometry, Part A* **2016**, *89A* (4), 325−327.

(24) Bajgiran, K. R.; Darapaneni, P.; Melvin, A. T.; Dorman, J. A. Effects of Weak Electric Field on the Photoluminescence Behavior of Bi3+-Doped YVO4:Eu3+ Core-Shell Nanoparticles. *J. Phys. Chem. C* **2019**, *123* (20), 13027−13035.
(25) Wilchek, M.; Bayer, E. A. APPLICATIONS OF AVIDIN-BIOTIN TECHNOLOGY - LITERATURE SURVEY. *Methods Enzymol.* **1990**, *184*, 14−45.
(26) Goldman, E. R.; Balighian, E. D.; Mattoussi, H.; Kuno, M. K.; Mauro, J. M.; Tran, P. T.; Anderson, G. P. Avidin: A natural bridge for quantum dot-antibody conjugates. *J. Am. Chem. Soc.* **2002**, *124* (22), 6378−6382.
(27) Tamura, T.; Hamachi, I. Chemistry for Covalent Modification of Endogenous/Native Proteins: From Test Tubes to Complex Biological Systems. *J. Am. Chem. Soc.* **2019**, *141* (7), 2782−2799.
(28) Richard, J. P. Protein Flexibility and Stiffness Enable Efficient Enzymatic Catalysis. *J. Am. Chem. Soc.* **2019**, *141* (8), 3320−3331.
(29) Qu, X. M.; Wang, S. P.; Ge, Z. L.; Wang, J. B.; Yao, G. B.; Li, J.; Zuo, X. L.; Shi, J. Y.; Song, S. P.; Wang, L. H.; Li, L.; Pei, H.; Fan, C. H. Programming Cell Adhesion for On-Chip Sequential Boolean Logic Functions. *J. Am. Chem. Soc.* **2017**, *139* (30), 10176−10179.
(30) Darapaneni, P.; Kizilkaya, O.; Wang, Z.; Dorman, J. A. Weak Field Tuning of Transition-Metal Dopant Hybridization in Solid Hosts. *J. Phys. Chem. C* **2018**, *122* (39), 22699−22708.
(31) Liu, Y. S.; Zhou, S. Y.; Tu, D. T.; Chen, Z.; Huang, M. D.; Zhu, H. M.; Ma, E.; Chen, X. Y. Amine-Functionalized Lanthanide-Doped Zirconia Nanoparticles: Optical Spectroscopy, Time-Resolved Fluorescence Resonance Energy Transfer Biodetection, and Targeted Imaging. *J. Am. Chem. Soc.* **2012**, *134* (36), 15083−15090.
(32) Oh, E.; Hong, M. Y.; Lee, D.; Nam, S. H.; Yoon, H. C.; Kim, H. S. Inhibition assay of biomolecules based on fluorescence resonance energy transfer (FRET) between quantum dots and gold nanoparticles. *J. Am. Chem. Soc.* **2005**, *127* (10), 3270−3271.
(33) Ju, Q.; Tu, D. T.; Liu, Y. S.; Li, R. F.; Zhu, H. M.; Chen, J. C.; Chen, Z.; Huang, M. D.; Chen, X. Y. Amine-Functionalized Lanthanide-Doped KGdF4 Nanocrystals as Potential Optical/Magnetic Multimodal BioProbes. *J. Am. Chem. Soc.* **2012**, *134* (2), 1323−1330.
(34) Hildebrandt, N.; Spillmann, C. M.; Algar, W. R.; Pons, T.; Stewart, M. H.; Oh, E.; Susumu, K.; Diaz, S. A.; Delehanty, J. B.; Medintz, I. L. Energy Transfer with Semiconductor Quantum Dot Bioconjugates: A Versatile Platform for Biosensing, Energy Harvesting, and Other Developing Applications. *Chem. Rev.* **2017**, *117* (2), 536−711.
(35) Zhang, Z.; Shikha, S.; Liu, J.; Zhang, J.; Mei, Q.; Zhang, Y. Upconversion Nanoprobes: Recent Advances in Sensing Applications. *Anal. Chem.* **2019**, *91* (1), 548−568.
(36) Cao, S.; Li, Z.; Zhao, J.; Chen, M.; Ma, N. Rational Engineering a Multichannel Upconversion Sensor for Multiplex Detection of Matrix Metalloproteinase Activities. *Acs Sensors* **2018**, *3* (8), 1522−1530.
(37) Howes, P. D.; Chandrawati, R.; Stevens, M. M. Colloidal nanoparticles as advanced biological sensors. *Science* **2014**, *346* (6205), 53.
(38) Wu, Y. F.; Tilley, R. D.; Gooding, J. J. Challenges and Solutions in Developing Ultrasensitive Biosensors. *J. Am. Chem. Soc.* **2019**, *141* (3), 1162−1170.
(39) Moreno, M.; Barriuso, M. T.; Aramburu, J. A. THE DEPENDENCE OF 10DQ UPON THE METAL-LIGAND DISTANCE, R, FOR TRANSITION-METAL COMPLEXES - WHAT IS ITS MICROSCOPIC ORIGIN. *Int. J. Quantum Chem.* **1994**, *52* (4), 829−835.

https://dx.doi.org/10.1021/acssensors.9b02204
ACS Sens. XXXX, XXX, XXX−XXX